Bulletin of JSME, Vol. 28, No. 244, October 1985

Paper No. 84—0146

Heat Transport of Powder as the Subject of Cryogenic Insulation*

(2nd Report, Heat Conduction under Vacuum)

by Eisyun TAKEGOSHI**, Yoshio HIRASAWA***

and Sadahisa IMURA****

In the present work, an investigation was made on the heat transport through insulation powder evacuated under high vacuum, in which an aluminium powder was added for radiation shield. Experiments on heat flux in the powder were carried out from room temperature down to liquefied helium temperature, which enabled us to examine the relation between the heat flux and temperature.

Furthermore, the general solution for total heat transfer for combined radiation and conduction proposed by Wang and Tien was applied to the powder, and was compared with the experimental results. We then quantitatively determined the roles of the contribution from both radiation and conduction and the effect of added aluminium powder, and investigated the basic heat transfer mechanisms in the powder at low temperatures such as extinction coefficient for radiation and contact conduction between particles.

Key Words : Thermophysical Properties, Thermal Conduction, Thermal Radiation, Low Temperature, Evacuated Powder Insulation

1. Introduction

In the previous report[1], a theoretical equation for the thermal conductivity of perlite and glass bubbles as a cryogenic insulation powder was derived and it agreed well with the experiments at any temperature and any gas pressure. In the present report, exclusively the heat transport in case that the insulation powder is evacuated at high vacuum is investigated.

Since the heat conduction by gas becomes very small at high vacuum, the heat transfer in the powder consists of the following two mechanisms, namely the solid conduction due to the contact between particles and the thermal radiation through the void space in the powder. In this study, many experiments on the relation between heat flux through the powder and absolute temperature are carried out from room temperature down to liquefied helium temperature. Powder specimens used in these experiments are perlite and glass bubbles employed in the previous study and silica employed anew. Experiments in which aluminium powder are added to these powders as a radiation shield material are also carried out.

The general solution for total heat transfer for combined radiation and conduction proposed by Wang and Tien[2] is applied to these powders and the result is compared with the experiments. Thus the fundamental characteristics of the heat transport in the powder at low temperatures such as radiation, contact conduction and the effect of added aluminium powder are investigated.

2. Experimental Specimens

The characteristics of employed powders are shown in Table 1. As the perlite and glass bubbles, two kinds of powders with different densities and different particle sizes were prepared. For the silica, a kind of powder was prepared. The description of the perlite and glass bubbles is omitted because it has been given in the previous report. The silica is made from anhydrous silicic acid with high purity and its particle size is much smaller than the other two powders. A moisture is hardly contained in the powder. The powder density ρ in Table 1 is a measured value under the condition that the specimens are packed in

Table 1 Characteristics of experimental specimens

Specimen	Size of particle mm	Average dia. of particle Dp mm	Density of powder ρ kg/m^3	Average porosity ϵ
Perlite F	1.2 -0.15	0.50	61 - 64	0.977
〃 C_2	1.4 - 1.0	1.4	143 - 148	0.946
Glass bubbles				
〃 B15	0.13-0.02	0.056	About 80	0.969
〃 B37	〃	0.036	〃 210	0.919
Silica	-	0.007	〃 64	0.971

* Received 23rd April, 1984.

** Associate Professor, Faculty of Engineering, Toyama University. Gofuku 3190, Toyama.

*** Assistant, Faculty of Engineering, Toyama University

**** Professor, Faculty of Engineering, Toyama University

the apparatus. The porosity ϵ is calculated from the average value of ρ, where the true densities of perlite, glass bubbles and silica are assumed to be 2700, 2600 and 2200 kg/m^3, respectively. In addition, experiments in which an aluminium powder was added to the powders of Table 1 were also done. The average sizes of the aluminium powder are 0.1 and 0.06 mm. The former is added to the perlite and the latter is added to the glass bubbles and silica. The added rates of the aluminium powder are 5, 20 and 50 % by weight.

3. Experimental Equipment

In this study, in addition to the devices (a) and (b) employed in the previous study[1], the device (c) in which the measurement down to liquefied helium temperature is possible is employed. The explanation of the devices (a) and (b) is omitted since it has been given in the previous report. As shown in Fig. 1, the measuring principle of the device (c) is the cylindrical absolute method with a steady heat flow such as in both the devices (a) and (b). In the device (c), the insulation with a double Dewar vessel is employed in order to use liquefied helium. The size of the outer Dewar vessel ⑩ is 120 mm inside diameter and 800 mm length. The size of the inner Dewar vessel ⑦ is 100 mm outside diameter, 80 mm inside diameter and 850 mm length. The specimen vessel ⑫, which is the main body of the device, is made of brass pipe of 36 mm inside diameter and 190 mm length and designed smaller than the ones of the devices (a) and (b). The main heater ⑬ is made of brass pipe of 14 mm outside diameter and 160 mm length. The cap of the specimen vessel is soldered with the stainless pipe ⑪ (15 mm inside diameter and 0.5 mm thickness) and the upside of the pipe is connected to the vacuum flange. The evacuation of the specimen vessel is carried out through the pipe and the lead wires for measuring are taken out through the pipe. In this device, subheaters at both ends of the main heater are not set and a correction[3] is made for the effect of the end. The temperature of the main heater was measured by a cryogenic thermocouple(Au+0.07At.%Fe-Chromel) soldered to the heater.

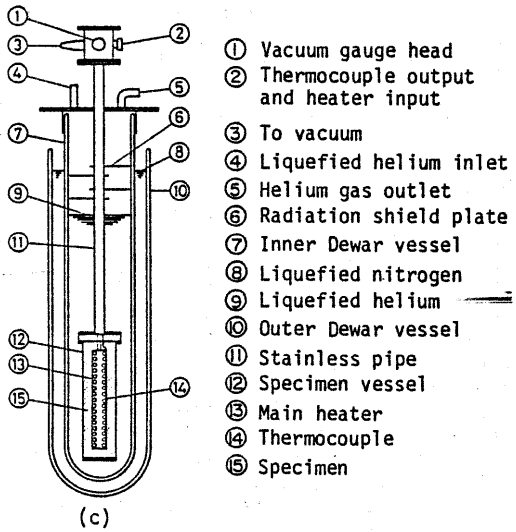

Fig. 1 Outline of experimental device at very low temperatures

The experimental procedure is as follows. A powder specimen is put into the specimen vessel and the cap is soldered with Wood metal. Thereafter, the specimen vessel is evacuated to attain a gas pressure of about 0.1 Pa at room temperature for many hours. Next, it is precooled with liquefied nitrogen and after it is put into the inner Dewar vessel, a liquefied helium is poured into the inner Dewar vessel. In a pre-experiment, since the evaporation volume of the liquefied helium has been about 50 cm^3 per hour, it is possible to continue the experiment for about 50 hours. In the experiment, after the electric current was supplied to the main heater to maintain a given temperature and the device was allowed to attain a steady state, then measurements of the electromotive force in the thermocouple and of the electric power to the main heater were done three times every 30 minutes and their average values were used for calculation. The measurements were started from the lowest temperature and continued up to about 200 K at every 10-30 K. The time taken to attain the steady state was 2-3 hours.

In these experiments the thermal conductivity is very small since the powder is evacuated to high vacuum. Accordingly, the heat inflow through the lead wires of the main heater and thermocouple causes an important error in the measurements at low temperature unlike in usual measurements. In all the devices (a), (b) and (c), the wires with as small diameter and low conductivity as possible were employed to reduce the heat inflow. Further the error in the conductivity due to the heat inflow was determined by a preliminary experiment to within about 10 %. This correction, therefore, was not done for the calculation of thermal conductivity. Further, when powders transparent to radiation are used in experiments it is known that the emissivity of the wall of the specimen vessel and main heater affects the experimental value [refer to Eq. (7)]. However, since the powders in this experiment were not supposed to be so transparent, the emissivity was not considered. We consider that the experimental error in these devices is within about 10 % at room temperature but is somewhat larger than this at low temperature because of the heat inflow described above and so on.

4. Result and Consideration

4.1 Effect of temperature on thermal conductivity under vacuum

In the previous report[1], the effective thermal conductivity λe for the powder containing a gas was represented by

the following equation:

$$\lambda_e=\varepsilon'(\lambda_g'+\alpha_r D_p)+\frac{1-\varepsilon'-\delta'}{\frac{1}{\lambda_g'/\phi+\alpha_r D_p}+\frac{1-\phi}{\lambda_p}}+\delta'\lambda_p \quad \cdots\cdots(1)$$

The explanation of the symbol is omitted since it has been done in the previous report. Equation (1) agreed well with the measurements for the powder of perlite and glass bubbles at atmospheric and low pressures. If Eq. (1) is applied under vacuum, it is approximated to the following equation in case of $1/\alpha_r Dp >> (1-\phi)/\lambda p$ (it is valid in this experiment) because the thermal conductivity of the gas becomes zero:

$$\lambda_e^0=(1-\delta')\alpha_r D_p+\delta'\lambda_p \quad \cdots\cdots(2)$$

where λ_e^0 is the effective thermal conductivity of the powder under vacuum, λ_p is the effective thermal conductivity of a particle constituting the powder, δ' is the effective contact area rate for solid conduction, α_r is the heat transfer coefficient for thermal radiation and Dp is particle diameter. The first term of the right side in Eq. (2) is concerned with radiation and the second term is concerned with the conduction due to the contact between particles. Thus Eq. (1) can be divided into the radiation and conduction terms under vacuum. For simplification, we assume $\delta'\lambda_p=\delta\lambda_s$ using the effective contact area rate δ based on the thermal conductivity λ_s of solid. Then Eq. (2) becomes the following equation as $\delta'<<1$ is considered:

$$\lambda_e^0=\alpha_r D_p+\delta\lambda_s \quad \cdots\cdots(3)$$

where α_r is represented by the following equation for the function of absolute temperature T:

$$\alpha_r=4\sigma\phi_r T^3=0.226\phi_r(T/100)^3\,[\mathrm{W/(m^2\cdot K)}] \quad \cdots\cdots(4)$$

and σ is Stefan-Boltzmann constant and ϕr is known as the radiation exchange factor which is a function of the form and arrangement of particles and emissivity ϵr. In the previous study, it was defined as $\phi r=1/(2/\epsilon r-1)$ based on a parallel plate model. ϕr is ordinarily smaller than unity. Here, we assume that the thermal conductivity λs of solid is approximately proportional to 2/3th power of T. For example, if the thermal conductivity of glass is employed for the solid of the perlite and glass bubbles and is represented by the following equation based on the conductivity at room temperature:

$$\lambda_s=0.0244\,T^{2/3}\,[\mathrm{W/(m\cdot K)}] \quad \cdots\cdots(5)$$

it agrees with the reference[4] within a deviation of about 10% in the range of 10-300 K. Therefore, Eq. (3) can be approximated as follows:

$$\lambda_e^0=0.226\phi_r(T/100)^3 D_p+0.0244\,T^{2/3}\delta \quad \cdots\cdots(6)$$

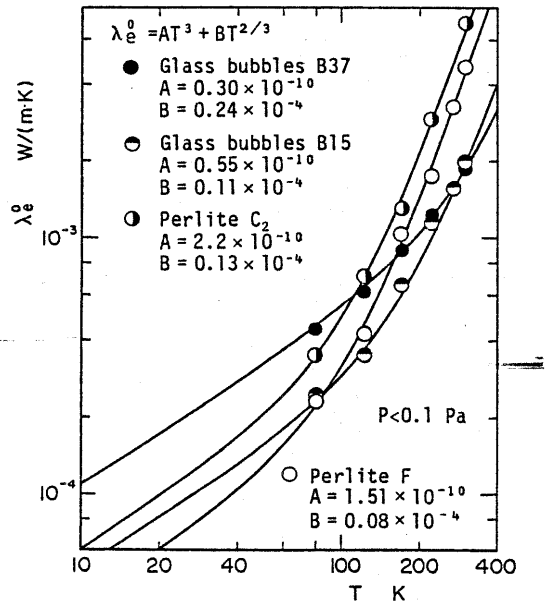

Fig. 2 Relation between effective thermal conductivity and temperature

Figure 2 shows the relation between λ_e^0 and T for the perlite and glass bubbles. Here, the temperature T is an arithmetic average when the temperature difference between inner and outer surfaces of the powder is set at about 10 °C. The marks o in the figure denote the experimental values, but some of them are estimated values with no pressure dependence which is extrapolated from the experiment for the relation between the thermal conductivity and pressure, because the pressure dependence of λ_e^0 in some specimens holds at about 0.1 Pa which is the lower limit of pressure in this experiment. The curves in Fig. 2 approximate experimental values by assuming that Eq. (6) can be applied. The coefficients A and B of T are also shown in this figure. λ_e^0 gradually increases with an increasing T at low temperatures and rapidly increases at high temperatures. This is because the contact conduction between particles is effective at low temperatures but the thermal radiation relatively increases with an increasing temperature. As the perlite F and C_2 are compared, λ_e^0 of C_2 is larger than that of F at all temperatures. This means that both the contact conduction and radiation of C_2 are larger than those of F because both the density and particle size are larger than those of F. In the glass bubbles, λ_e^0 of B37 is larger than that of B15 at low temperature under the effect of contact conduction due to the larger density of B37 than B15, but λ_e^0 of B15 becomes larger at high temperature on account of the contribution of radiation due to the larger size of B15 than B37. Next, comparing the perlite and glass bubbles, both λ_e^0 do not differ so much at low temperature in the case of similar densities such as the perlite F and glass bubbles B15, but λ_e^0 of the perlite F becomes clearly larger with an increasing temperature. This can be understood from the fact that the diameter Dp of the perlite F is far larger than that of the glass bubbles B37 (over ten times).

Table 2 shows the values of ϕr and δ which are obtained by comparing Eq. (6) with the coefficients A and B in Fig. 2. The values of ϕr are closer to unity for the perlite but are considerably larger

Table 2 Experimental values of ϕ_r and δ

Specimen	ϕ_r	δ
Perlite F	1.33	3.28×10^{-4}
〃 C_2	0.70	5.32×10^{-4}
Glass bubbles B15	4.35	4.50×10^{-4}
〃 B37	3.68	9.84×10^{-4}

than unity for the glass bubbles. The reason is thought as follows. Equation (6) is derived from a cell model in which the particle diameter Dp is employed as a unit path for radiation. Therefore, if the particle is an opaque material for radiation, ϕ_r shall become closer to unity. However, since a long radiation path through the particle exists if it is somewhat transparent, Dp already may not be fit as the unit path of the model for radiation. Accordingly, it seems that ϕ_r larger than unity for the glass bubbles is caused by the above mentioned fact. Thus the glass bubbles may be a little transparent. On the other hand, the values of δ in Table 2 are about 10^{-4}-10^{-3}, which are considerably small values. For example, they are smaller by about one order than $\delta=6.3\times10^{-3}$, which has been obtained by authors[5] for a packed bed of solid glass spheres at room temperature. Thus it is understood that the effect of the contact conduction becomes smaller because the particle itself of the powder in this experiment is porous.

4.2 Application of quasi-homogeneous theory for heat flow in powder

In the section 4.1 it was shown that the radiation exchange factor ϕ_r determined from the cell model agreed qualitatively with the experimental value, but quantitatively did not agree with the experiment in the case of glass bubbles due to the long radiation path. In this section, we examine the practical case of a large temperature difference between the inside and outside of powder, which is often encountered in a cryogenic insulation. Many experiments on the heat flux in powder are compared with a heat transfer theory in which the powder is regarded as a semitransparent quasi-homogeneous material. Wang and Tien[2] proposed a general solution for a total heat flux q for the plate type medium of thickness L under the condition of combined conduction and radiation. Namely,

$$q=\frac{(3/4)\lambda_d\beta(T_1-T_2)+\nu^2\sigma(T_1^4-T_2^4)}{\frac{3}{4}\tau+\left[\frac{(3/8)+(1-\varepsilon_{r_1})/3}{(\lambda_d\beta/4\sigma T_1^3)+2\varepsilon_{r_1}/3}\right]+\left[\frac{(3/8)+(1-\varepsilon_{r_2})/3}{(\lambda_d\beta/4\sigma T_2^3)+2\varepsilon_{r_2}/3}\right]} \quad \cdots\cdots(7)$$

where T_1 and T_2 are the temperatures of two walls which sandwich the medium, ϵ_{r_1} and ϵ_{r_2} are the emissivities of the walls, σ is Stefan-Boltzmann constant; and λ_d, ν, β and τ are the thermal conductivity, the refractive index, the extinction coefficient and the optical thickness of the medium, respectively. Here, holds the relation of $\tau=\beta L$. In Eq. (7), if τ is sufficiently large, q is given by the following equation since the first and second terms in the denominator are ignored:

$$q=\frac{4\nu^2\sigma(T_1^4-T_2^4)}{3\beta L}+\frac{\lambda_d(T_1-T_2)}{L} \quad \cdots\cdots(8)$$

It is found that Eq. (8) is divided into the radiation and conduction terms.

As q in Eq. (8) is the solution for the case of plate type medium, $r\ln(r_2/r_1)$ must be employed instead of the thickness L of the powder when this equation is applied to the walls of a double cylinder such as used in this device. Then, Eq. (8) becomes

$$q_1=\frac{4\nu^2\sigma(T_1^4-T_2^4)}{3\beta r_1\ln(r_1/r_2)}+\frac{\lambda_d(T_1-T_2)}{r_1\ln(r_1/r_2)} \quad \cdots\cdots(9)$$

where q_1 is the heat flux at the inside wall and r_1 and r_2 are the radii of the inside and outside walls, respectively. λ_d in Eq. (9) has temperature dependence because it is proportional to the contact conduction between particles. Therefore, we simply assume λ_d as the following equation:

$$\left.\begin{aligned}&\lambda_d=0.0244\,T_m^{2/3}\delta\\&\text{(Perlite, Glass bubbles)}\\&\lambda_d=0.0308\,T_m^{2/3}\delta\ \text{(Silica)}\end{aligned}\right\} \quad \cdots(10)$$

which is proportional to the two-thirds power of the temperature such as shown in Eq. (5). However, in this case the average temperature $T_m[=(T_1+T_2)/2]$ is employed because of a large temperature difference between the inside and outside walls. λ_d for silica in Eq. (10) is determined from the thermal conductivity of fused quartz at room temperature.

Figures 3-5 show the relation between the heat flux q_1 at inner wall and the temperature difference $\Delta T(=T_1-T_2)$, in which the device (b) is employed and the temperature T_2 of the outer wall is kept at that(77K) of liquefied N_2 and the temperature T_1 of inner wall is changed up to room temperature. In these figures, the experiments in which aluminium powder is added or not added are compared in order to examine the effect of aluminium. The added rates of aluminium are 5, 20 and 50 wt%. The curves in these figures approximate the experimental values to the form of Eq. (9). The coefficients A' and B' for the approximated curves are shown in each figure. In the case of the perlite F in Fig. 3, q_1 does not change so much with the added rate of aluminium. This means that the insulation performance is not improved so much by the added aluminium because the perlite is considerably opaque to radiation. For the glass bubbles B15 in Fig. 4, q_1 clearly changes with the added rate of aluminium. At ΔT=223 K, q_1 is greatest for Aℓ 0 % and is smallest for Aℓ 20 wt%, whose ratio is about twice. Namely, it seems that the effect of the added aluminium appears clearly. As for the coefficients A' and B', A' decreases with an increasing added rate of aluminium up to Aℓ 20 wt% but becomes nearly equal at Aℓ 20 and 50 wt%. Therefore, it is likely that the effect of radiation shield increases up to Aℓ 20 wt%. This corresponds with the fact that

the powder of the glass bubbles is somewhat transparent to radiation as mentioned concerning ϕ_r in section 4.1. On the other hand, B' decreases slightly up to Aℓ 20 wt% but increases at 50 wt%, because the contact conduction increases as the added rate of aluminium exceeds a certain limit. Figure 5 shows the case of the silica. It seems that the effect of the added aluminium is similar to the case of the glass bubbles.

Next, when A' of the perlite, glass bubbles and silica in the non-added case of aluminium are compared, A' of the silica is largest though the particle size of the silica is much smaller than others. This suggests that the silica is most transparent to radiation among these three kinds of powders. However, the effect of the added aluminium on the silica is not so large as shown in Fig. 5, because the average size of the added aluminium is 60 μm which is very large as compared with that(7 μm) of the silica and therefore the effect of radiation shield is small. Hunter et al.[6] have reported that the effect of radiation shield generally increases with a decrease in the particle size of added metal.

Figure 6 shows the relation between q_1 and ΔT measured with the device (c), in which the temperature T_2 of the outer wall is kept at liquefied helium temperature(4 K) and the temperature T_1 of the inner wall is changed arbitrarily up to about 200 K. The curves in this figure approximate the experimental values assuming that Eq. (9) is equally applicable. As the temperature T_2 is 4 K in this case, the contribution of radiation is considerably small at small ΔT(explain in Table 3). Accordingly, it may be understood that the difference of q_1 for each specimen at small ΔT is mainly caused by contact conduction rather than by radiation.

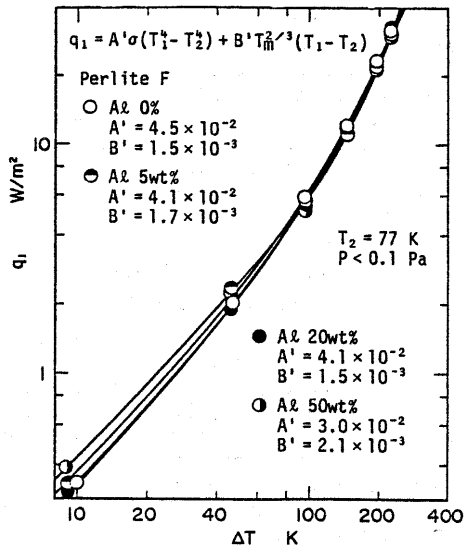

Fig. 3 Relation between heat flux at inner surface and temperature difference

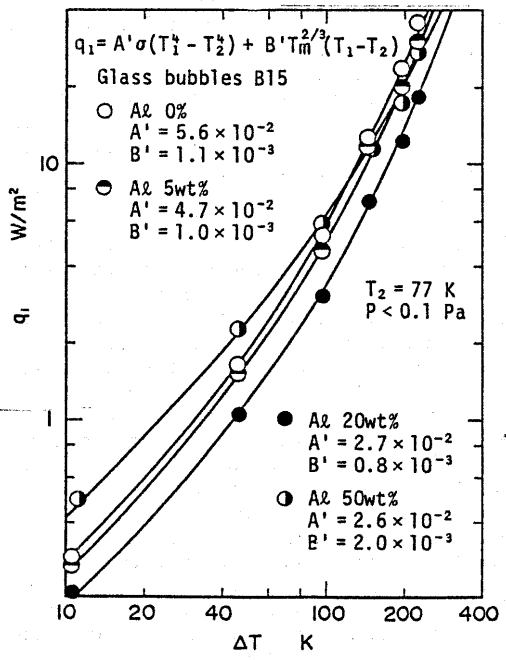

Fig. 4 Relation between heat flux at inner surface and temperature difference

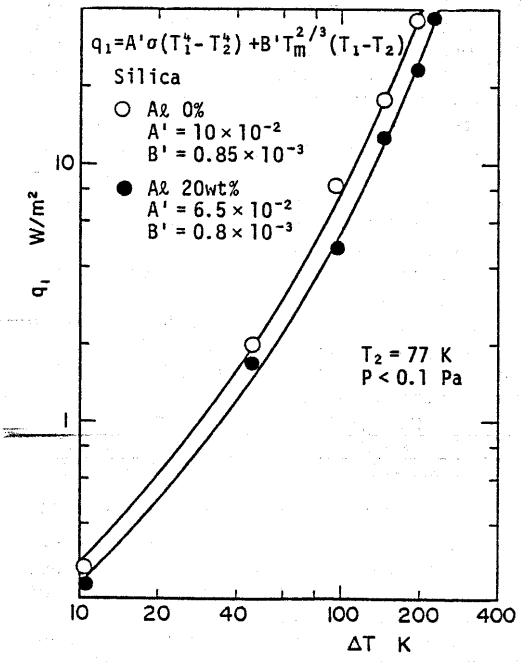

Fig. 5 Relation between heat flux at inner surface and temperature difference

4.3 Effect of radiation and contact conduction on heat transfer in powder

Table 3 shows the rate of the heat flux due to the radiation contribution to the total heat flux q_1, which is calculated from the coefficients A' and B' in Figs. 3-6. For example in the case of T_2=77 K for the perlite F, the radiation contribution is 65 % at ΔT=223 K(T_1=300 K) but it is 17 % at ΔT=10 K, while in

the case of T_2=4 K, it is considerably smaller. As a whole, it is found that the radiation contribution in the powder is above 50 % at T_1 of about room temperature but it decreases rapidly with a decrease in ΔT. When the cases of 20 wt% added and non-added aluminium to the glass bubbles are compared, the radiation contribution does not much differ at each T_1 for both cases of T_2=77 and 4 K. However, the heat flux q_1 for the specimen of Aℓ 20 wt% is clearly small as shown in Figs. 4 and 6. This means that a proper aluminium is effective to reduce both the radiation and contact conduction.

Table 4 shows the extinction coefficient β for radiation for each specimen, which is determined by comparing the coefficient A' in Figs. 3-6 with the first term in right side of Eq. (9). Here, the refractive index ν is assumed to be 1.1, and r_1 and r_2 are 11 and 25 mm in the experiment of T_2=77 K and 7 and 18 mm in the experiment of T_2=4 K, respectively. It is found in this table that β for the silica is smallest when the specimens of Aℓ 0 % are compared. The silica therefore seems to be most transparent to radiation among these three powders. On the other hand, when the change in β is observed with the added aluminium it increases on the whole with an increase of aluminium and the effect of radiation shield appears. Furthermore comparing the cases of T_2=77 and 4 K, the difference is not so large. Cunnington and Tien[7] have obtained β=48 cm^{-1} for the glass bubbles with no aluminium from the experiments at T_2=77 K and T_1=270-350 K and it is equivalent to this experiment. They have also done an experiment on the glass bubbles coated with aluminium and have obtained the values of β=260-350 cm^{-1}. In general, it is known that β is about 5-500 cm^{-1} for the insulation powder with low density[8].

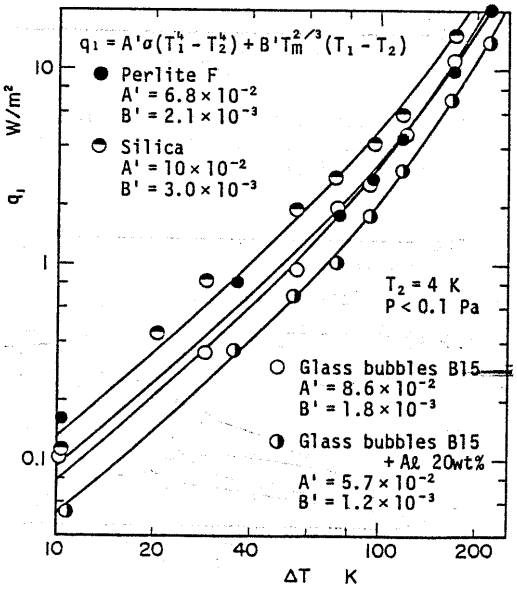

Fig. 6 Relation between heat flux at inner surface and temperature difference

Table 5 shows the values of the contact area rate δ which are calculated by comparing the coefficient B' with the second term in right side of Eq. (9) and by employing Eq. (10). The values of δ are in the range of 10^{-4}-10^{-3} for all the specimens. These roughly correspond to δ shown in Table 2. In the case of glass bubbles, it is found that δ becomes smallest at Aℓ 20 wt%, namely contact conduction is smallest. Comparing the cases of T_2=77 and 4 K, there is no significant difference between them.

4.4 Mean effective thermal conductivity of powder

Figures 7-10 show the mean effective thermal conductivity λ^0_{em} between temperatures T_1 and T_2 calculated from heat flux q_1. The calculation of λ^0_{em} was carried out using the following:

$$\lambda^0_{em} = q_1 r_1 \ln(r_2/r_1)/(T_1 - T_2) \quad \cdots\cdots\cdots\cdots (11)$$

In Figs. 7-10, λ^0_{em} generally do not so much increase at small ΔT since contact conduction is dominant, but increase rapidly with an increasing ΔT because the heat flux due to radiation is proportional to T^4. As explained already for the heat

Table 3 Rate of radiation contribution to total heat flux

Specimen	ΔT K / T_2 K	Radiation contribution %			
		10	73	150	223
Perlite F	77	17	32	51	65
	4	0.16	7.0	27	48
Glass bubbles B15	77	25	44	64	76
	4	0.24	9.9	36	58
Glass bubbles B15 + Aℓ20wt%	77	18	34	54	68
	4	0.24	9.9	35	57
Silica	77	44	65	80	88
	4	0.17	7.2	28	49

Table 4 Extinction coefficient for radiation

Specimen	Temp. T_2 K	Extinction coefficient β cm^{-1}			
		Aℓ 0%	5 wt%	20 wt%	50 wt%
Perlite F	77	40	44	44	60
	4	36	-	-	-
Glass bubbles B15	77	32	38	66	68
	4	28	-	43	-
Silica	77	18	-	27	-
	4	24	-	-	-

Table 5 Effective area rate for contact conduction

Specimen	Temp. T_2 K	Contact area rate δ			
		Aℓ 0%	5 wt%	20 wt%	50 wt%
Perlite F	77	$5.6^{\times 10^{-4}}$	$6.3^{\times 10^{-4}}$	$5.6^{\times 10^{-4}}$	$7.8^{\times 10^{-4}}$
	4	5.7	-	-	-
Glass bubbles B15	77	4.1	3.7	3.0	7.4
	4	4.9	-	3.3	-
Silica	77	2.5	-	2.7	-
	4	6.4	-	-	-

flux in Figs. 3-6, λ^0_{em} for the glass bubbles and silica decrease with an addition of aluminium.

Table 6 shows λ^0_{em} of each specimen in two cases that the boundary temperature T_1 equals 300 K(room temperature) and T_2 equals 77 K(liquefied N_2) and that T_1 equals 77 K and T_2 equals 4 K(liquefied He), which are usually encountered in the cryogenic insulation. From the table, it is found that λ^0_{em} are roughly the order of about 10^{-3} W/(m·K) between 300 and 77 K and about 10^{-4} W/(m·K) between 77 and 4 K. As these values are compared with that of a multilayer insulation[9], they are larger than that by about 1 or 2 power. However, the powder insulation has often an advantage because it is thermally isotropic, simpler to install, less expensive and practically reliable.

5. Conclusions

The heat transport in insulation powder evacuated under high vacuum was investigated experimentally at low temperatures and the following results were obtained.

(1) The heat flux q in the powder under vacuum can be divided into the terms of radiation and conduction as shown theoretically by Wang and Tien and can be indicated in the form of Eq. (8).

(2) When aluminium is added to the powder, the heat flux in the powder for the glass bubbles and silica can be decreased though that for the perlite can not be decreased. The effect of the added aluminium is largest at 20 wt% with the glass bubbles.

(3) The radiation contribution to total heat flux is over about 50 % at the hot boundary of room temperature, but is below several percent at the hot boundary of very low temperatures under 77 K. Namely, the heat flux in the powder at low temperatures is caused by contact conduction rather than by radiation.

(4) The extinction coefficient β for radiation is about 18-68 cm^{-1} for the powders employed in the present work. It

Table 6 Mean effective thermal conductivity of several specimens for cryogenic insulation

Specimen	Boundary temp. T_1 K	T_2 K	λ^0_{em} W/(mK)	Al powder
Perlite F	300	77	0.00132	Null
	300	77	0.00130	20 wt%
	77	4	0.00015	Null
Glass bubbles B15	300	77	0.00142	Null
	300	77	0.00077	20 wt%
	77	4	0.00017	Null
Silica	300	77	0.00193	Null
	300	77	0.00144	20 wt%
	77	4	0.00026	Null

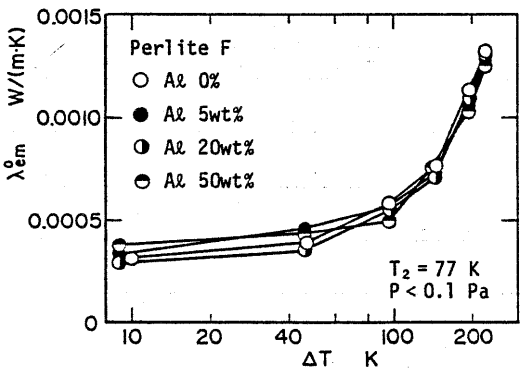

Fig. 7 Relation between mean effective thermal conductivity and temperature difference

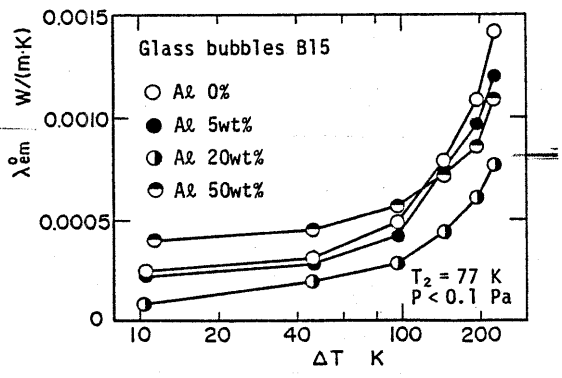

Fig. 8 Relation between mean effective thermal conductivity and temperature difference

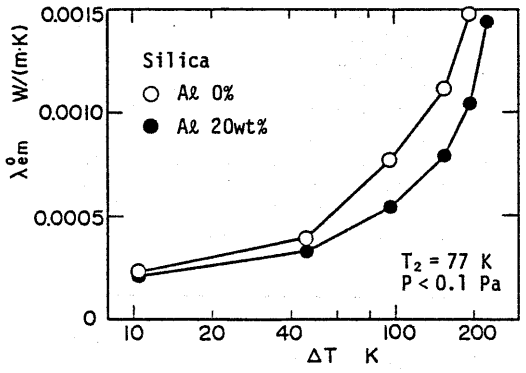

Fig. 9 Relation between mean effective thermal conductivity and temperature difference

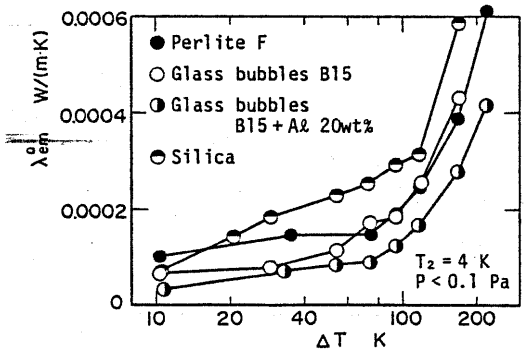

Fig. 10 Relation between mean effective thermal conductivity and temperature difference

is smallest for the silica and is largest for the perlite and also increases with an increasing added aluminium.

(5) The coefficient δ to show the area rate for the contact conduction between particles is about 10^{-4}-10^{-3} for all the specimens.

References

[1] Takegoshi, E., et al., Bull. Japan Soc. Mech. Engrs., Vol. 27, No. 233(1984-11), p. 2455.
[2] Wang, L. S. and Tien, C. L., Int. J. Heat Mass Transf., Vol. 10, No. 10(1967), p. 1327.
[3] Nukiyama, S. and Itahashi, Y., J. Japan Soc. Mech. Engrs. (in Japanese), Vol. 39, No. 227(1936-3), p. 135.
[4] Touloukian, Y. S., et al., TPRC Data Series, Vol. 2(1970), p. 922, IFI/Plenum.
[5] Imura, S. and Takegoshi, E., Heat Transfer Japanese Research, Vol. 3, No. 4(1974), p. 13.
[6] Hunter, B. J., et al., Advan. Cryog. Eng., Vol. 5(1960), p. 146.
[7] Cunnington, G. R. and Tien, C. L., Advan. Cryog. Eng., Vol. 18(1973), p. 103.
[8] Tien, C. L. and Cunnington, G. R., Advan. Heat Transf., Vol. 9(1973), p. 349.
[9] Tien, C. L. and Cunnington, G. R., Cryogenics, Vol. 12(1972), p. 419.